Physics of Wave Processes and Radio Systems
2024, vol. 27, no. 3, pp. 81–90

DOI 10.18469/1810-3189.2024.27.3.81-90
UDC 621.371.334:537.874.6
Original Research

Received 2 April 2024
Accepted 6 May 2024
Published 30 September 2024

Plasmonic antennas based on rectangular graphene nanoribbons with controlled polarization of terahertz and infrared radiation

Galina S. Makeeva

Penza State University
40, Krasnaya Street,
Penza, 440026, Russia

Abstract – **Background.** To develop new terahertz wireless communication systems with high throughput and transmission speeds, such as 6G and above, effective control of the polarization direction of emitted terahertz waves is necessary, but most methods are technologically complex and expensive. The implementation of terahertz antennas and devices based on 2D materials such as graphene solves the problem associated with developing effective control. **Aim.** Study of the possibility of controlling the polarization of terahertz and IR radiation of plasmonic antennas based on rectangular graphene nanoribbons by changing the chemical potential (application of an external electric field). **Methods.** This important scientific problem related to the design of terahertz antennas can largely be solved by simulation using the electrodynamic simulation program CST MWS 2023. **Results.** Plasmon terahertz antennas based on rectangular graphene nanoribbons were chosen as the object of analysis and the possibility of emitting waves of two orthogonal polarizations was shown. Methods have been identified for controlling the polarization of terahertz and IR radiation from such antennas, based on the selection of operating frequencies corresponding to the resonances of the modes of surface plasmon-polaritons, and the application of metallization to the dielectric substrate. **Conclusion.** The ability to control the polarization of terahertz and IR radiation makes it possible to create both new elements of plasmonic antenna arrays and new communication technologies, including future 6G networks.

Keywords – plasmonic antennas; rectangular graphene nanoribbons; polarization; plasmon resonance; radiation pattern.

Introduction

New wireless communication standards such as 6G require higher bandwidth than current technologies can provide. The terahertz (THz) frequency band is highly promising for high-speed wireless communication networks [1] because it can significantly boost transmission rates compared to ultrahigh-frequency (UHF) bands, especially in 6G Wi-Fi networks [2].

Two-dimensional (2D) materials such as graphene play a crucial role in efficient polarization control in THz devices and antennas. With its unique optoelectronic properties and high doping potential, graphene has become key material in plasmonic antennas [3–7] and THz polarizers [8–11]. It exhibits high carrier mobility and consistently absorbs light across wavelengths. Graphene properties can be tuned by adjusting its chemical potential (Fermi level) via electrical gating and chemical doping. Graphene is chemically and structurally stable owing to the strong covalent bonds among carbon atoms, which enable it to support long-lived and tunable plasmon resonances when excited by THz and infrared (IR) radiation [3].

Graphene analogs of standard metal antennas exhibit better emitting properties [4–7]. This is largely attributed to graphene's excellent surface conductivity, which is highly responsive to changes in chemical potential when a bias voltage is applied [12]. Such dynamic conductivity control is expected to support operations at terabit-per-second speeds [3].

New THz, ultra-high-performance, and ultra-precise communication systems require efficient control of the polarization direction of the emitted waves. However, most available methods are complex and expensive [2].

The ST MWS and HFSS simulation software packages can solve important problems related to the design of microwave devices, antennas, and phased antenna arrays [13; 14].

This study uses the CST Microwave Studio electromagnetic simulation system to investigate how the polarization of terahertz and IR radiation emitted by plasmonic antennas made of rectangular graphene nanoribbons can be controlled. This control can be achieved by changing the chemical potential by applying an external electric field.

✉ radiotech@pnzgu.ru (*Galina S. Makeeva*)

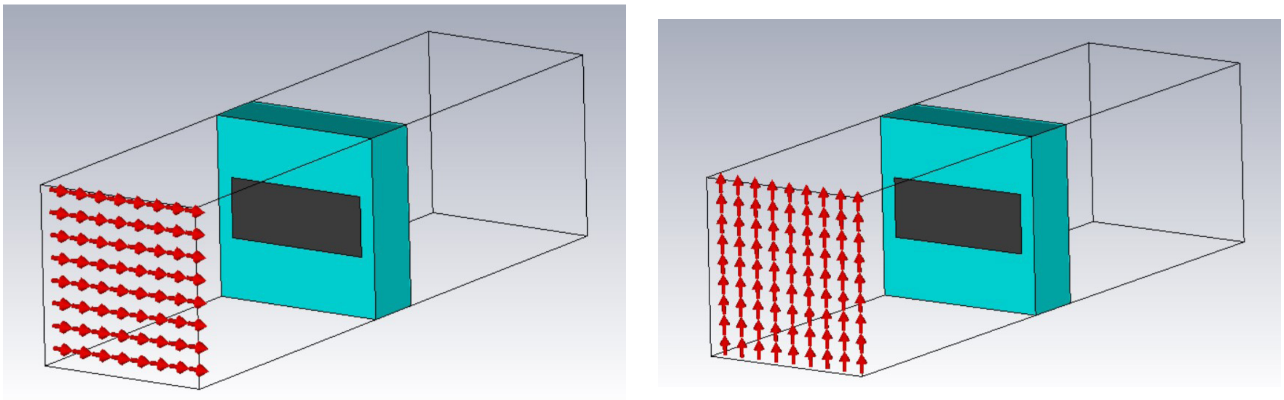

a *b*

Fig. 1. Excitation of a plasmonic antenna with a rectangular graphene nanoribbon using a waveguide port: *a* – s-polarized and *b* – p-polarized TEM. Simulated in CST MWS 2023

Рис. 1. Модели возбуждения плазмонной антенны на основе прямоугольной графеновой наноленты TEM-волной s-поляризации (*а*) и p-поляризации (*б*) с помощью волноводного порта в программном комплексе CST MWS 2023

1. Simulation of plasmonic antenna behavior in a rectangular graphene nanoribbon excited by s- and p-polarized TEM wave under chemical potential change

Fig. 1 illustrates the CST MWS 2023 [15] models of excitation of a plasmonic antenna with a rectangular graphene nanoribbon can be excited by a normally incident TEM wave. In these models, the wave is either s-polarized (Fig. 1, *a*) or p-polarized (Fig. 1, *b*) using a waveguide port. The antenna model features a rectangular graphene nanoribbon with dimensions of length (*l*) and width (*w*) (Fig. 1) installed on a dielectric substrate made of silicon dioxide (SiO_2), characterized by a dielectric constant ($\varepsilon = 2{,}2$), and with dimensions *a*, *b*, and *h*.

Fig. 1 also depicts the orientation of the incident TEM wave's electric field strength vector **E** relative to the graphene nanoribbon. For an s-polarized wave, vector **E** is oriented along the wide side of the graphene nanoribbon (Fig. 1, *a*), whereas for a p-polarized wave, vector E aligns with the narrow side (Fig. 1, *b*).

We used the models presented in Fig. 1 to address the electrodynamic problem using CST Microwave Studio 2023 employing finite integration in the time domain [3].

We calculated an element of the scattering matrix $|S_{12}|$ for a graphene plasmonic antenna excited by s- and p-polarized TEM waves across the THz, far-IR, and mid-IR ranges, considering different values of the graphene's chemical potential μ_c.

Fig. 1 also depicts the orientation of the incident TEM wave's electric field strength vector **E** relative to the graphene nanoribbon. For an s-polarized wave, vector **E** is oriented along the wide side of the graphene nanoribbon (Fig. 1, *a*), whereas for a p-polarized wave, vector E aligns with the narrow side (Fig. 1, *b*).

We used the models presented in Fig. 1 to address the electrodynamic problem using CST Microwave Studio 2023 employing finite integration in the time domain [3].

We calculated an element of the scattering matrix $|S_{12}|$ for a graphene plasmonic antenna excited by s- and p-polarized TEM waves across the THz, far-IR, and mid-IR ranges, considering different values of the graphene's chemical potential μ_c.

Fig. 2 displays the frequency responses of the scattering matrix element $|S_{12}|$, which represents thewave transmission coefficient, for a plasmonic antenna with a rectangular graphene nanoribbon. The nanoribbon dimensions are the following: $w = 1$ μm, $l = 2{,}5$ μm, $a = b = 3$ μm, $h = 1$ μm). Furthermore. the chemical potential values are the following: $\mu_{c1} = 0{,}3$ eV, $\mu_{c2} = 0{,}7$ eV, $\mu_{c3} = 1$ eV. The antenna was excited by a TEM wave, which exhibited s-polarization (Fig. 2, *a*) and p-polarization (Fig. 2, *b*). The graphene properties considered in this simulation are $T = 300$ K and $\tau = 1$ ps.

The simulation results (Fig. 2) indicate that frequency shifts and the minima of the transmission coefficient μ_c vary with changes in the graphene chemical potential $|S_{12}|$. The transmission coefficient $|S_{12}|$ minima (Fig. 2, *a*, *b*) result from the maxima of the absorption coefficient *P* in graphene. These min-

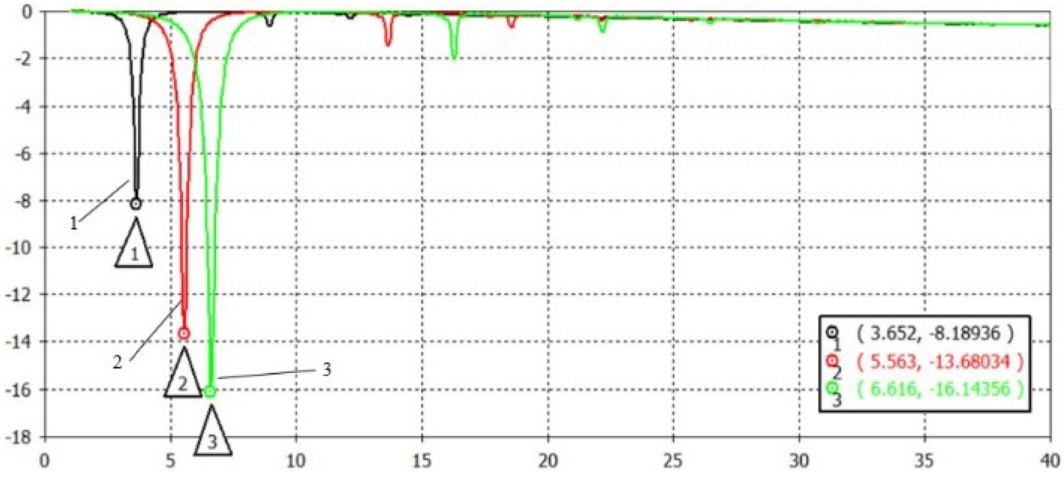

a

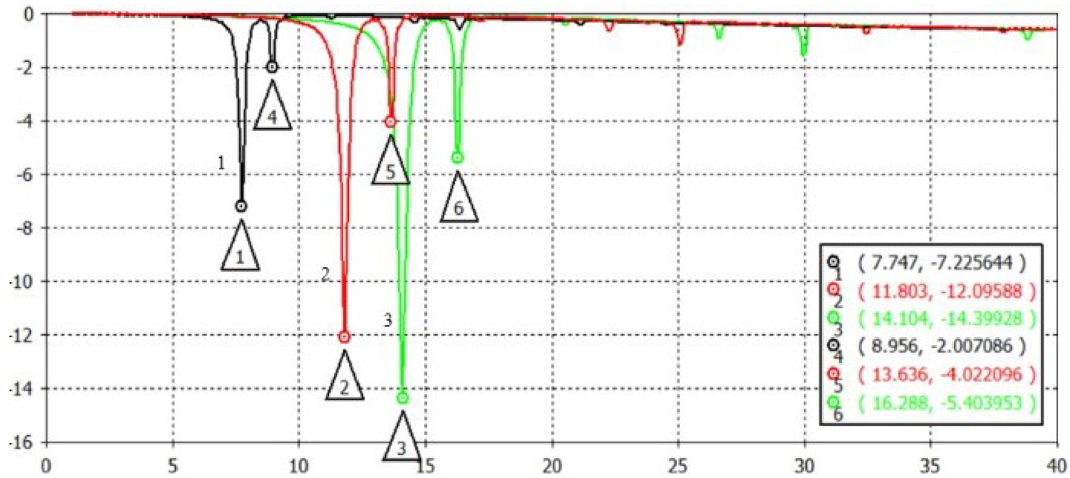

b

Fig. 2. Frequency responses of the scattering matrix element $|S_{12}|$ within a plasmonic antenna containing a rectangular graphene nanoribbon at different chemical potentials μ_c in the THz, far and mid-IR ranges: *a* – s-polarization; *b* – p-polarization of the incident TEM wave; curve *1* – $\mu_{c1} = 0{,}3$ eV, *2* – $\mu_{c2} = 0{,}7$ eV, *3* – $\mu_{c3} = 1$ eV; $w = 1$ μm, $l = 2{,}5$ μm, $b = 3$ μm, $h = 1$ μm

Рис. 2. Частотные зависимости элемента матрицы рассеяния $|S_{12}|$ плазмонной антенны на основе прямоугольной графеновой наноленты для различных значений химического потенциала μ_c в ТГц, дальнем и среднем ИК-диапазонах: *а* – s-поляризация; *б* – p-поляризация падающей ТЕМ-волны; кривая 1 – $\mu_{c1} = 0{,}3$ эВ, 2 – $\mu_{c2} = 0{,}7$ эВ, 3 – $\mu_{c3} = 1$ эВ; $w = 1$ мкм, $l = 2{,}5$ мкм, $a = b = 3$ мкм, $h = 1$ мкм

ima align with the plasmon resonances [16] that occur at frequencies f_{res} driven by the excited main and higher modes of surface plasmon polaritons (SPPs) [11]. These resonant frequencies $f_{res}^{s,p}$ are influenced by the incident wave polarization [11].

For an s-polarized excitation TEM wave, in which the surface electric current resonates along the wide side of the rectangular graphene nanoribbon, longitudinal plasmon resonance occurs [11]. In this case, the first resonant frequency f_1^{s1} is determined by the main mode of SPPs (Fig. 2, *a*). At this frequency, the electric current density j_s on the graphene surface reaches its peak, leading to maximum absorption. For a p-polarized excitation TEM wave, a transverse resonance of the surface electric current j_s occurs along the narrow side of the rectangular graphene nanoribbon [11], enabling resonance frequencies f_{res}^{p} to be higher than f_{res}^{s} for the s-polarization (Fig. 2, *b*). We observed several resonant frequencies corresponding to the nearest higher SPP modes for both s-polarization (Fig. 2, *a*) and p-polarization (Fig. 2, *b*). In a rectangular graphene nanoribbon, the longitudinal SPP resonance occurs at s-polarization (Fig. 2, a), whereas the transverse SPP resonance appears at p-polarization (Fig. 2, *b*), each at different frequencies.

The table lists the estimated scattering matrix element $|S_{12}|$ at the resonance frequencies $f_{res}^{s,p}$ of the main and second-order SPP modes excited by an s- and p-polarized TEM wave for different chemical potentials μ_c (0,3, 0,7, 1 eV).

Table. Calculated values of the scattering matrix element $|S_{12}|$ at the resonant frequencies $f_{рез}^{s,p}$ of the main and second SPP modes excited by an s- and p-polarized TEM wave for different chemical potentials μ_c

Таблица. Расчетные значения элемента матрицы рассеяния $|S_{12}|$ на резонансных частотах $f_{рез}^{s,p}$ основной и второй мод ППП, возбуждаемых ТЕМ-волной s- и p-поляризации, для различных значений химического потенциала μ_c

μ_c, eV	$f_{рез}^{s1}$, THz	S_{11}, dB	$f_{рез}^{p1}$, THz	S_{11}, dB	$f_{рез}^{p2}$, THz	S_{11}, dB
0,3	3,652	−8,18936	7,747	−7,22564	8,967	−2,00709
0,7	5,563	−13,68034	11,803	−12,09588	13,636	−4,0221
1	6,616	−16,14356	14,104	−14,39928	16,288	−5,40395

2. Simulation of THz and IR radiation polarization control for plasmonic antennas with rectangular graphene nanoribbons

Fig. 3 illustrates the simulation results from CST MWS 2023. We modeled the directivity pattern (DP) of a plasmonic graphene antenna on a dielectric substrate and examined the distribution of the surface electric current density vector $\mathbf{j}_s$ on the graphene nanoribbon at the resonant frequencies f_1^{s1}, f_2^{s1}, associated with the main SPP mode. This occurs when the antenna is excited by an s-polarized TEM wave, considering different chemical potentials of 0,3, 0,7, 1 eV.

Fig. 3 – 3.1–3.3, *a–c* illustrate how the frequency of a plasmonic graphene antenna can be tuned, or frequency-swept, at resonant frequencies f_{res}^{s1} corresponding to the main SPP mode when excited by an s-polarized TEM wave in the terahertz range, as the chemical potential μ_c varies from 0,3 to 1 eV by applying an external electric field.

At the resonant frequencies of the main SPP mode, excited by an s-polarized TEM wave, a resonance of the electric current is generated by the standing SPP half-wave along the wide side of the rectangular nanoribbon [11]. This results in a half-wave distribution of the surface electric current j_s along the length of the rectangular graphene nanoribbon, peaking at the center (Fig. 3 – 3.1–3.3, *d*). The resulting 3D DP of the radiation produced by this half-wavelength (half of the SPP wavelength) electric emitter is toroidal (Fig. 3 – 3.1–3.3, *c*). The axis of the 2D DP in the equatorial plane aligns with the longitudinal emitting current (Fig. 3 – 3.1–3.2, *b*). The DP in the *E*-plane, which depends on θ at $\varphi = 0°$), matches that of a half-wave symmetric vibrator [17]. In the E-plane (depending on θ at $\varphi = 90°$), the DP forms a circle (Fig. 3 – 3.1–3.3, *a*).

As the chemical potential μ_c increases, the surface electric current density rate j_s on the graphene nanoribbon increases (Fig. 3 – 3.1–3.3, *d*). This occurs because the q-value of the resonance decreases, leading to a higher absorption coefficient in graphene [11], which in turn boosts the emitting efficiency of the plasmonic graphene antenna (Fig. 3 – 3.1–3.3, *c*).

For comparison, Fig. 4 presents the simulated DP of a plasmonic antenna with a rectangular graphene nanoribbon on a metalized dielectric substrate, maintaining identical dimensions ($w = 1$ μm, $l = 2{,}5$ μm, $a = b = 3$ μm, $h = 1$ μm). This is presented at the resonant frequency f_3^{s1} that matches the main SPP mode, equal to $f_3^{s1} = 5{,}252$ THz when excited by an s-polarized TEM wave at a given chemical potential of $\mu_c = 1$ eV.

The comparison of the DPs for plasmonic antennas containing rectangular graphene nanoribbons on dielectric substrates (Fig. 3 – 3.3) and metalized substrates (Fig. 4) substrates at resonant frequencies f_3^{s1} corresponding to the main SPP mode indicates that the directivity axis, and therefore, the polarization plane of the half-wave THz radiation (half of the SPP wavelength) emitted by the electric emitter, is rotated by 90° in the latter case.

Plasmonic antennas containing rectangular graphene nanoribbons on dielectric and metalized substrates emit THz waves with two orthogonal polarizations. This means that by applying metallization to the dielectric substrate, we can control the polarization of the THz radiation.

Fig. 5 presents the simulation results from CST MWS 2023, showing the DP of a plasmonic graphene antenna on a dielectric substrate. It also depicts the distribution of the surface electric current density vector $\mathbf{j}_s$ on the graphene nanoribbon at resonant frequencies f_1^{p1}, f_1^{p1}, f_1^{p1} corresponding to the main SPP mode, when the antenna is excited by a p-polarized TEM wave at different chemical potentials (0,3, 0,7, 1 eV).

Fig. 5 – 5.1–5.3, *a-c* demonstrate the capability of tuning the operating frequency of a plasmonic

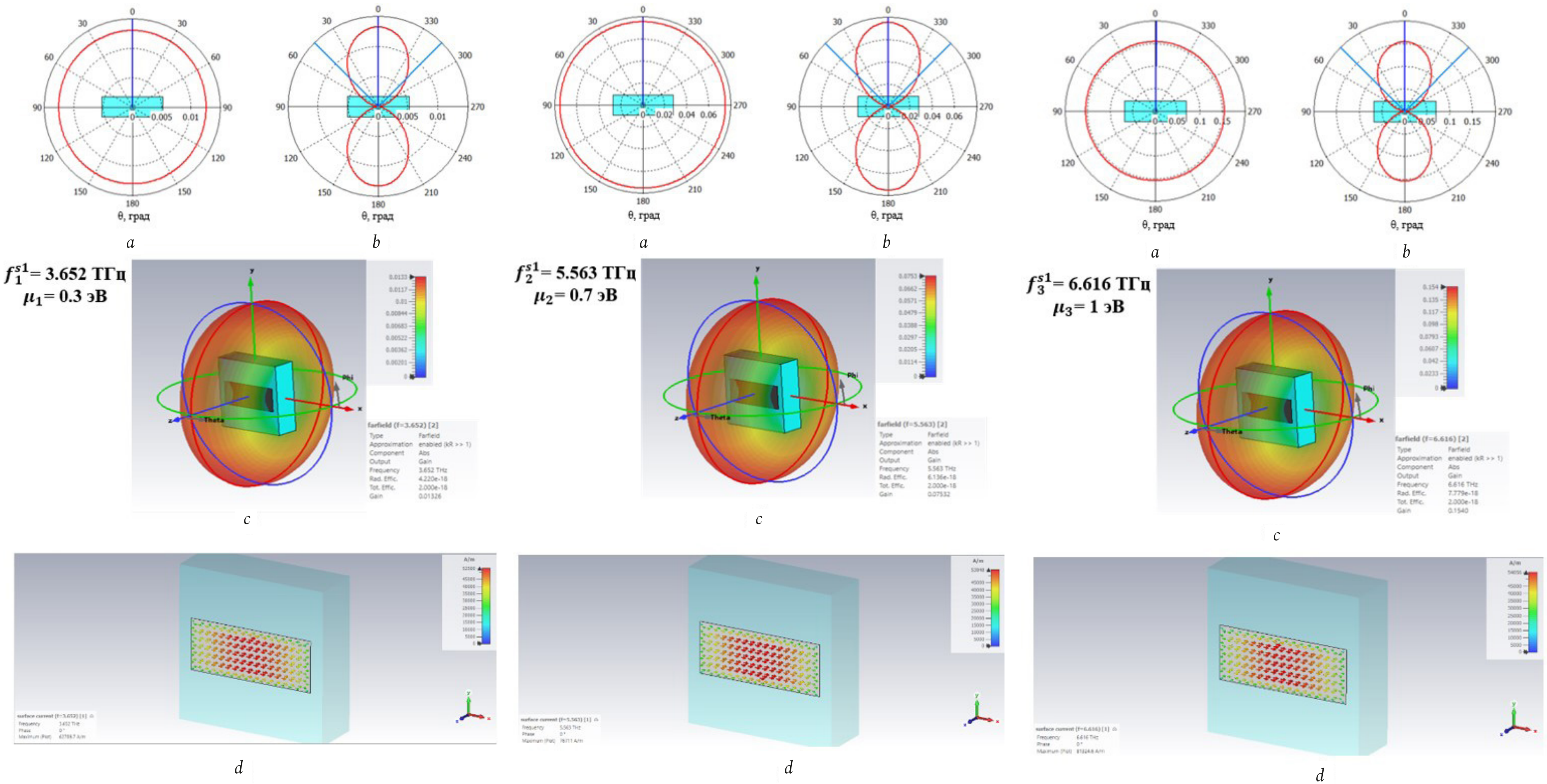

3.1 3.2 3.3

Fig. 3. DP of a plasmonic antenna with a rectangular graphene nanoribbon on a dielectric substrate at resonance frequencies $f_{рез}^{s1}$ corresponding to the main SPP mode when excited by an s-polarized TEM wave. A frequency sweep in the THz range is performed as the chemical potential μ_c changes. 2D RP in the E-plane (depending on θ, $\varphi = 90°$) (*a*), in the E-plane (depending on θ, $\varphi = 0°$) (*b*) in the polar (*a*, *b*) and 3D RP in the spherical (*c*) coordinate systems and the distribution of the surface electric current density vector on the graphene nanoribbon (*d*); 3.1 – f_1^{s1} = 3,652 THz, μ_{c1} = 0,3; 3.2 – f_2^{s1} = 5,563 THz, eV; 3.3 – f_3^{s1} = 6,616 THz, μ_{c3} = 1 eV. The radiation level and the surface current density are visualized using a color map in the digital edition

Рис. 3. ДН плазмонной антенны на основе прямоугольной графеновой наноленты на диэлектрической подложке на резонансных частотах $f_{рез}^{s1}$ основной моды ППП при s-поляризации возбуждающей ТЕМ-волны и сканирование по частоте в ТГц-диапазоне при изменении значения химического потенциала μ_c: 2D ДН в *E*-плоскости (в зависимости от θ, $\varphi = 90°$) (*а*), в *E*-плоскости (в зависимости от θ, $\varphi = 0°$) (*б*) в полярной (*а*, *б*) и 3D ДН в сферической (*в*) системах координат и распределение вектора плотности поверхностного электрического тока $\mathbf{j}_s$ на графеновой наноленте (*г*); 3.1 – f_1^{s1} = 3,652 ТГц, μ_{c1} = 0,3; 3.2 – f_2^{s1} = 5,563 ТГц, μ_{c2} = 0,7 эВ; 3.3 – f_3^{s1} = 6,616 ТГц, μ_{c3} = 1 эВ; интенсивность излучения и плотности поверхностного электрического тока j_s обозначены цветом в электронной версии статьи

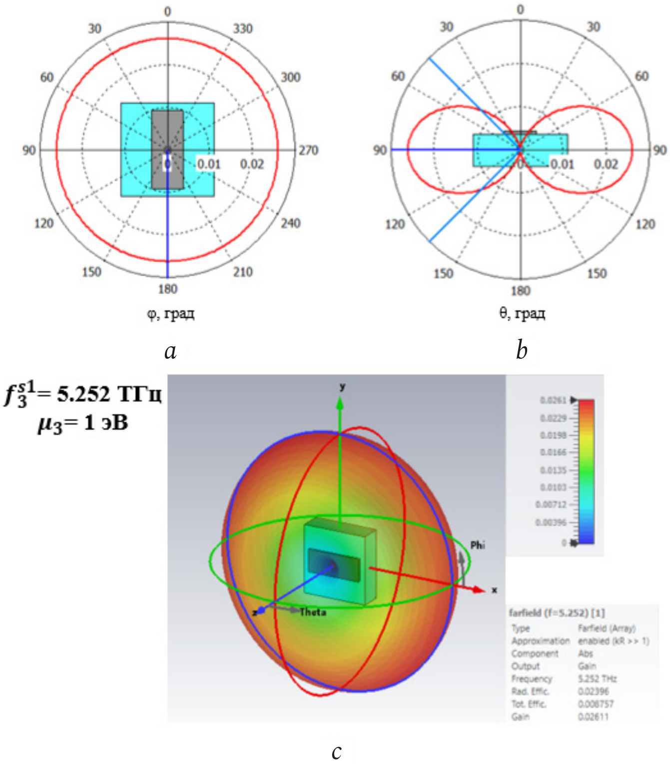

Fig. 4. DP of a plasmonic antenna with a rectangular graphene nanoribbon on a metalized dielectric substrate excited by an s-polarized TEM at the resonant frequency corresponding to the main SPP mode f_3^{s1} = 5,252 THz, μ_{c3} = 1 eV: 2D RP in the H-plane (depending on φ, θ = 90°) (*a*) and in the E-plane (depending on θ, φ = 90°) (*b*) in the polar (*a*, *b*) and 3D RP in the spherical (*c*) coordinate systems
Рис. 4. ДН плазмонной антенны на основе прямоугольной графеновой наноленты на металлизированной диэлектрической подложке при s-поляризации возбуждающей ТЕМ-волны на резонансной частоте основной моды ППП f_3^{s1} = 5,252 ТГц, μ_{c3} = 1 эВ: 2D ДН в *H*-плоскости (в зависимости от φ, θ = 90°) (*а*) и в *E*-плоскости (в зависимости от θ, φ = 90°) (*б*) в полярной (*а*, *б*) и 3D ДН в сферической (*в*) системах координат

graphene antenna (frequency scanning), allowing it to scan from the THz range to the far and mid-IR ranges. This frequency tuning is achieved at resonant frequencies f_{res}^{p1} of the main SPP mode when the antenna is excited by a p-polarized wave. The tuning is facilitated by varying chemical potential μ_c between 0,3 and 1 eV using an external electric field).

At the resonant frequencies of the main SPP mode, excited by an s-polarized wave, a resonance of the electric current is generated by the standing SPP half-wave along the wide side of the rectangular nanoribbon [11]. This results in a half-wave distribution of the surface electric current j_s along the length of the rectangular graphene nanoribbon, peaking at the center (Fig. 5 – 5.1–5.3, *d*). The resulting 3D DP for the radiation emitted by this half-wavelength (half of the SPP wavelength) electric emitter is toroidal (Fig. 5 – 5.1–5.3, *c*). The axis of the 2D DP in the equatorial plane aligns with the longitudinal emitting current (Fig. 5 – 5.1–5.3, *d*). In the *E*-plane (depending on θ at φ = 90°), the DP matches that of a half-wave symmetric vibrator [17] (Fig. 5 – 5.1–5.2, *a*), and in the *E*-plane, (depending on θ at φ = 0°) it forms a circle (Fig. 5 – 5.1–5.3, *b*).

The comparison of the DPs at the resonance frequencies of the main SPP mode f_3^{s1} = 6,616 THz for s-polarization (Fig. 3 – 3.3) and f_3^{p1} = 14,104 THz for p-polarization (Fig. 5 – 5.3) indicates that the directivity axis is parallel to the longitudinal emitting current in the first case and to the transverse emitting current in the second case. Therefore, the polarization plane of the half-wave THz radiation (half of the SPP wavelength) from the electric emitter [17] rotates 90° in the meridian plane.

A plasmonic antenna with rectangular graphene nanoribbons on a dielectric substrate can emit waves with two orthogonal polarizations. This happens when the resonance frequency shifts from the SPP mode f_{res}^{s} for s-polarization to the SPP mode f_{res}^{p} for p-polarization of the exciting TEM wave. Consequently, the polarization of THz/IR radiation from such antennas can be controlled by selecting the signal frequency depending on the type of plasmon

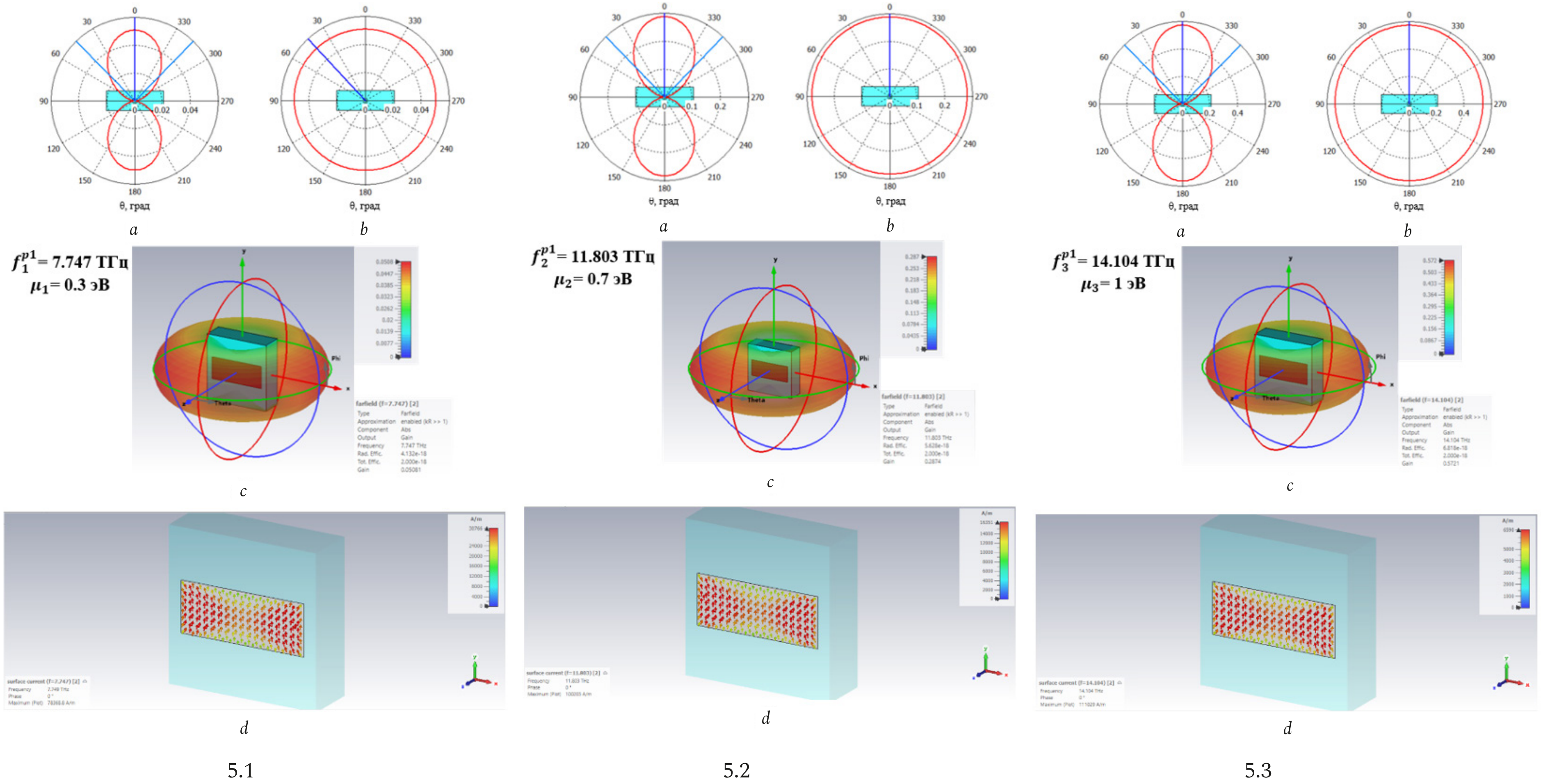

Fig. 5. TDP of a plasmonic antenna containing a rectangular graphene nanoribbon on a dielectric substrate at the resonance frequencies $f_{рез}^{p1}$ corresponding to the main SPP mode when excited by a p-polarized TEM wave and frequency sweep in the THz range as the chemical potential μ_c changes. 2D RP in the E-plane (depending on θ, $\varphi = 90°$) (*a*), in the E-plane (depending on θ, $\varphi = 0°$) (*b*) in the polar (*a*, *b*) and 3D RP in the spherical (*c*) coordinate systems and the distribution of the surface electric current density vector $\mathbf{j}_s$ on a rectangular graphene nanoribbon (*d*); 5.1 – $f_1^{p1} = 7{,}747$ THz, $\mu_{c1} = 0{,}3$; 5.2 – $f_2^{p1} = 11{,}803$ THz, $\mu_{c2} = 0{,}7$ eV; 5.3 – $f_3^{p1} = 14{,}104$ THz, $\mu_{c3} = 1$ eV. The radiation level and the surface current density j_s are visualized using a color map in the digital edition

Рис. 5. ДН плазмонной антенны на основе прямоугольной графеновой наноленты на диэлектрической подложке на резонансных частотах $f_{рез}^{p1}$ основной моды ППП при p-поляризации возбуждающей TEM-волны и сканирование по частоте в ТГц, дальнем и среднем ИК-диапазонах при изменении значения химического потенциала μ_c: 2D ДН в *E*-плоскости (в зависимости от θ, $\varphi = 90°$) (*а*), в *E*-плоскости (в зависимости от θ, $\varphi = 0°$) (*б*) в полярной (*а*, *б*) и 3D ДН в сферической (*в*) системах координат и распределение вектора плотности поверхностного электрического тока $\mathbf{j}_s$ на прямоугольной графеновой наноленте (г); 5.1 – $f_1^{p1} = 7{,}747$ ТГц, $\mu_{c1} = 0{,}3$; 5.2 – $f_2^{p1} = 11{,}803$ ТГц, $\mu_{c2} = 0{,}7$ эВ; 5.3 – $f_3^{p1} = 14{,}104$ ТГц, $\mu_{c3} = 1$ эВ; интенсивность излучения и плотности поверхностного электрического тока j_s обозначены цветом в электронной версии журнала resonance, either longitudinal or transverse, in the rectangular graphene nanoribbon.

Conclusion

The simulation results reveal that plasmonic antennas with rectangular graphene nanoribbons can emit THz/IR waves with two orthogonal polarizations. We identified methods to control the polarization of these waves by selecting signal frequencies that align with the plasmon resonances of SPP modes and through metallization of the dielectric substrate.

This ability to control THz/IR radiation enables the creation of both new plasmonic antenna array elements [18] and new communication technologies, including future 6G networks [2]. These advancements will support energy-efficient communication, enable cognitive radio networks that can intelligently change channels, and facilitate in-band full-duplex technology that can double the bandwidth [2].

References

1. T. Nagatsuma, "Terahertz technologies: present and future," *IEICE Electronics Express*, vol. 8, no. 14, pp. 1127–1142, 2011, doi: https://doi.org/10.1587/elex.8.1127.
2. D. Khusyainov et al., "Polarization control of THz emission using spin-reorientation transition in spintronic heterostructure," *Scientific Reports*, vol. 11, no. 1, p. 697, 2021, doi: https://doi.org/10.1038/s41598-020-80781-5.
3. J. D. Cox and F. J. Abajo, "Nonlinear graphene nanoplasmonics," *Accounts of Chemical Research*, vol. 52, no. 9, pp. 2536–2547, 2019, doi: https://doi.org/10.1021/acs.accounts.9b00308.
4. Y. Wu et al., "Graphene-based Yagi–Uda antenna with reconfigurable radiation patterns," *AIP Advances*, vol. 6, no. 6, p. 065308, 2016, doi: https://doi.org/10.1063/1.4953916.
5. S. A. Naghdehforushha and G. Moradi, "High directivity plasmonic graphene-based patch array antennas with tunable THz band communications," *Optik*, vol. 168, pp. 440–445, 2018, doi: https://doi.org/10.1016/j.ijleo.2018.04.104.
6. E. L. Isam et al., "Design and development of a graphene-based reconfigurable patch antenna array for THz applications," *Frequenz*, vol. 77, no. 3, pp. 219–228, 2023, doi: https://doi.org/10.1515/freq-2022-0051.
7. G. Varshney et al., "A proximity coupled wideband graphene antenna with the generation of higher order TM modes for THz applications," *Optical Materials*, vol. 85, pp. 456–463, 2018, doi: https://doi.org/10.1016/j.optmat.2018.09.015.
8. G. S. Makeeva et al., "Mathematical modeling of controlled terahertz polarizers based on periodic 2D structures made of rectangular graphene nanoribbons," *Izvestiya vuzov. Povolzhskiy region. Fiziko-matematicheskie nauki*, no. 2 (34), pp. 203–216, 2015, url: https://cyberleninka.ru/article/n/matematicheskoe-modelirovanie-upravlyaemyh-polyarizatorov-teragertsovogo-diapazona-na-osnove-periodicheskih-2d-struktur-iz. (In Russ.)
9. G. S. Makeeva, O. A. Golovanov, and R. A. Gorelov, "Methods and efficiency of control of dispersion of electromagnetic waves in the waveguiding structure based on carbon nanotube-graphene at terahertz and infrared frequency ranges," *Physics of Wave Processes and Radio Systems*, vol. 18, no. 4, pp. 24–33, 2015, url: https://journals.ssau.ru/pwp/article/view/7225. (In Russ.)
10. A. M. Lerer and G. S. Makeeva, "Reconfigurable terahertz polarizers and absorbers based on graphene metasurfaces," *2018 International Conference on Actual Problems of Electron Devices Engineering (APEDE)*, pp. 363–370, 2018, doi: https://doi.org/10.1109/APEDE.2018.8542192.
11. A. M. Lerer and G. S. Makeeva, "Polarization effects and resonant absorption during diffraction of terahertz waves on graphene metasurfaces," *Optika i spektroskopiya*, vol. 125, no. 6, pp. 838–843, 2018, doi: https://doi.org/10.21883/OS.2018.12.46948.257-18. (In Russ.)
12. O. A. Golovanov et al., "Calculation of efficiency of control of graphene conductivity by the external electric field at teraherz frequency range," *Physics of Wave Processes and Radio Systems*, vol. 18, no. 2, pp. 27–32, 2015, url: https://journals.ssau.ru/pwp/article/view/7311. (In Russ.)
13. A. A. Kurushin, *Designing Microwave Devices in CST Studio Suite*. Moscow: Solon-press, 2018. (In Russ.)
14. A. A. Kurushin and S. E. Bankov, *Modeling Antennas and Microwave Structures Using HFSS*. Moscow: Solon-press, 2018. (In Russ.)
15. CST Microwave Studio 2023. URL: https://www.3ds.com/products/simulia
16. O. A. Golovanov, G. S. Makeeva, and V. V. Varenitsa, "Mathematical modeling of diffraction of tem-wave on the periodic 2D structures of graphene micro-ribbons with finite length at terahertz frequency range," *Physics of Wave Processes and Radio Systems*, vol. 17, no. 4, pp. 17–25, 2014, url: https://journals.ssau.ru/pwp/article/view/7251. (In Russ.)
17. A. L. Drabkin and V. L. Zuzenko, *Antenna-Feeder Devices*. Moscow: Sovetskoe radio, 1961. (In Russ.)
18. N. N. Nefedov and G. S. Makeeva, "Electronic beam control and frequency scanning of a graphene antenna array in the terahertz and far-IR frequency ranges," *Technical Physics Letters*, vol. 49, no. 5, pp. 37–42, 2023, doi: https://doi.org/10.1134/S1063785023040028.

Information about the Author

Makeeva Galina Stepanovna, Doctor of Physical and Mathematical Sciences, Professor of the Department of Radio Engineering and Radioelectronic Systems, Penza State University, Penza, Russia. After graduating with honors in 1968 from the Penza Polytechnic Institute with a degree in Radio Engineering, she studied in the graduate school of LETI in 1969–1972. The academic degree of Candidate of Technical Sciences was awarded by the Dissertation Council of LETI in April 1973 and approved by the Higher Attestation Commission of the USSR in December 1973. Since 1973 she has been working at the Penza Polytechnic Institute, first as an assistant, and since 1974 as an associate professor (the academic title of associate professor in the Department of Radio Engineering was awarded by the Higher Attestation Commission of the USSR in 1977); since 1993 – Professor of the Department of Radio Engineering, Penza State Technical University. In 1997, she defended her doctoral dissertation in specialty 01.04.03 «Radiophysics, including quantum radiophysics» at the Dissertation Council of the Institute of Radio Engineering and Electronics of the Russian Academy of Sciences. The academic degree of Doctor of Physical and Mathematical Sciences was awarded by the Higher Attestation Commission of the Russian Federation on October10, 1997. In December 1997, she was awarded the academic title of Professor in the Department of Radio Engineering. In November 2000, she was elected a full member of the A.M. Prokhorov Academy of Engineering Sciences of the Russian Federation, Volga Region Branch.

Research interests: radiophysics, computational electrodynamics, electromagnetic field theory and numerical methods, nanoelectrodynamics, microwave and millimeter range devices and instruments, terahertz range components and devices, magnetic nanomaterials and nanostructures, graphene metamaterials and plasmonics, microwave photonics.

E-mail: radiotech@pnzgu.ru

Физика волновых процессов и радиотехнические системы
2024. Т. 27, № 3. С. 81–90

DOI 10.18469/1810-3189.2024.27.3.81-90
УДК 621.371.334:537.874.6
Оригинальное исследование

Дата поступления 2 апреля 2024
Дата принятия 6 мая 2024
Дата публикации 30 сентября 2024

Плазмонные антенны на основе прямоугольных графеновых нанолент с управляемой поляризацией терагерцового и инфракрасного излучения

Г.С. Макеева

Пензенский государственный университет
440026, Россия, г. Пенза,
ул. Красная, 40

Аннотация – **Обоснование.** Для развития новых терагерцовых систем беспроводной связи с высокой пропускной способностью и скоростью передачи, таких как 6G и выше, необходимо эффективное управление направлением поляризации излучаемых терагерцовых волн, однако большинство методов технологически сложные и дорогие. Реализация терагерцовых антенн и устройств на основе 2D-материалов, таких как графен, решает проблему, связанную с разработкой эффективного управления. **Цель.** Исследование возможности управления поляризацией терагерцового и ИК-излучения плазмонных антенн на основе прямоугольных графеновых нанолент с помощью изменения химического потенциала (приложением внешнего электрического поля). **Методы.** Эту важную научную проблему, связанную с проектированием терагерцовых антенн, во многом позволяет решить моделирование с помощью программы электродинамического моделирования CST MWS 2023. **Результаты.** В качестве объекта анализа выбраны плазмонные терагерцовые антенны на основе прямоугольных графеновых нанолент и показана возможность излучения волн двух ортогональных поляризаций. Выявлены способы управления поляризацией терагерцового, ИК-излучения таких антенн, основанные на выборе рабочих частот, соответствующих резонансам мод поверхностных плазмон-поляритонов, и нанесении металлизации на диэлектрическую подложку. **Заключение.** Возможность управления поляризацией терагерцового, ИК-излучения позволяет создавать как новые элементы плазмонных антенных решеток, так и новые коммуникационные технологии, в том числе будущих сетей 6G.

Ключевые слова – плазмонные антенны; прямоугольные графеновые наноленты; поляризация; плазмонный резонанс; диаграмма направленности.

radiotech@pnzgu.ru (*Макеева Галина Степановна*)

Список литературы

1. Nagatsuma T. Terahertz technologies: present and future // IEICE Electronics Express. 2011. Vol. 8, no. 14. P. 1127–1142. DOI: https://doi.org/10.1587/elex.8.1127
2. Polarization control of THz emission using spin-reorientation transition in spintronic heterostructure / D. Khusyainov [et al.] // Scientific Reports. 2021. Vol. 11, no. 1. P. 697. DOI: https://doi.org/10.1038/s41598-020-80781-5
3. Cox J.D., García de Abajo F.J. Nonlinear graphene nanoplasmonics // Accounts of Chemical Research. 2019. Vol. 52, no. 9. P. 2536–2547. DOI: https://doi.org/10.1021/acs.accounts.9b00308
4. Graphene-based Yagi–Uda antenna with reconfigurable radiation patterns / Y. Wu [et al.] // AIP Advances. 2016. Vol. 6, no. 6. P. 065308. DOI: https://doi.org/10.1063/1.4953916
5. Naghdehforushha S.A., Moradi G. High directivity plasmonic graphene-based patch array antennas with tunable THz band communications // Optik. 2018. Vol. 168. P. 440–445. DOI: https://doi.org/10.1016/j.ijleo.2018.04.104
6. Design and development of a graphene-based reconfigurable patch antenna array for THz applications / E.L. Isam [et al.] // Frequenz. 2023. Vol. 77, no. 3-4. P. 219–228. DOI: https://doi.org/10.1515/freq-2022-0051

7. A proximity coupled wideband graphene antenna with the generation of higher order TM modes for THz applications / G. Varshney [et al.] // Optical Materials. 2018. Vol. 85. P. 456–463. DOI: https://doi.org/10.1016/j.optmat.2018.09.015

8. Математическое моделирование управляемых поляризаторов терагерцового диапазона на основе периодических 2D-структур из прямоугольных нанолент графена / Г.С. Макеева [и др.] // Известия вузов. Поволжский регион. Физико-математические науки. 2015. № 2 (34). С. 203–216. URL: https://cyberleninka.ru/article/n/matematicheskoe-modelirovanie-upravlyaemyh-polyarizatorov-teragertsovogo-diapazona-na-osnove-periodicheskih-2d-struktur-iz

9. Макеева Г.С., Голованов О.А., Горелов Р.А. Способы и эффективность управления дисперсией электромагнитных волн в волноведущей структуре «углеродная нанотрубка – графен» в терагерцовом и инфракрасном диапазонах // Физика волновых процессов и радиотехнические системы. 2015. Т. 18, № 4. С. 24–33. URL: https://journals.ssau.ru/pwp/article/view/7225

10. Lerer A.M., Makeeva G.S. Reconfigurable terahertz polarizers and absorbers based on graphene metasurfaces // 2018 International Conference on Actual Problems of Electron Devices Engineering (APEDE). 2018. P. 363–370. DOI: https://doi.org/10.1109/APEDE.2018.8542192

11. Лерер А.М., Макеева Г.С. Поляризационные эффекты и резонансное поглощение при дифракции терагерцовых волн на графеновых метаповерхностях // Оптика и спектроскопия. 2018. Т. 125, № 6. С. 838–843. DOI: https://doi.org/10.21883/OS.2018.12.46948.257-18

12. Расчет эффективности управления проводимостью графена действием электрического поля в терагерцовом диапазоне частот / О.А. Голованов [и др.] // Физика волновых процессов и радиотехнические системы. 2015. Т. 18, № 2. С. 27–32. URL: https://journals.ssau.ru/pwp/article/view/7311

13. Курушин А.А. Проектирование СВЧ-устройств в CST Studio Suite. М.: Солон-пресс, 2018. 428 с.

14. Курушин А.А., Банков С.Е. Моделирование антенн и СВЧ-структур с помощью HFSS. М.: Солон-пресс, 2018. 280 с.

15. CST Microwave Studio 2023. URL: https://www.3ds.com/products/simulia

16. Голованов О.А., Макеева Г.С., Вареница В.В. Математическое моделирование дифракции ТЕМ-волны на периодических 2D-структурах из микролент графена конечной длины в терагерцовом диапазоне // Физика волновых процессов и радиотехнические системы. 2014. Т. 17, № 4. С. 17–25. URL: https://journals.ssau.ru/pwp/article/view/7251

17. Драбкин А.Л., Зузенко В.Л. Антенно-фидерные устройства. М.: Советское радио, 1961. 816 с.

18. Nefedov N.N., Makeeva G.S. Electronic beam control and frequency scanning of a graphene antenna array in the terahertz and far-IR frequency ranges // Technical Physics Letters. 2023. Vol. 49, no. 5. P. 37–42. DOI: https://doi.org/10.1134/S1063785023040028

Информация об авторе

Макеева Галина Степановна, доктор физико-математических наук, профессор кафедры радиотехники и радиоэлектронных систем Пензенского государственного университета, г. Пенза, Россия. После окончания с отличием в 1968 г. Пензенского политехнического института по специальности «Радиотехника» в 1969–1972 гг. обучалась в аспирантуре ЛЭТИ. Ученая степень кандидата технических наук присуждена Диссертационным советом ЛЭТИ в апреле 1973 г. и утверждена ВАК СССР в декабре 1973 г. С 1973 г. работает в Пензенском политехническом институте сначала в должности ассистента, с 1974 г. – доцента (ученое звание доцента по кафедре радиотехники присвоено ВАК СССР в 1977 г.); с 1993 г. – профессора кафедры радиотехники Пензенского государственного технического университета. В 1997 г. защитила докторскую диссертацию по специальности 01.04.03 «Радиофизика, включая квантовую радиофизику» в Диссертационном совете Института радиотехники и электроники РАН. Ученая степень доктора физико-математических наук присуждена ВАК РФ 10 октября 1997 г. В декабре 1997 г. присвоено ученое звание профессора по кафедре радиотехники. В ноябре 2000 г. избрана действительным членом Академии инженерных наук РФ им. А.М. Прохорова по Поволжскому отделению.

Область научных интересов: радиофизика, вычислительная электродинамика, теория электромагнитного поля и численные методы, наноэлектродинамика, устройства и приборы СВЧ- и миллиметрового диапазонов, компоненты и устройства терагерцового диапазона, магнитные наноматериалы и наноструктуры, графеновые метаматериалы и плазмоника, микроволновая фотоника.

E-mail: radiotech@pnzgu.ru